

Induced magnetism at interfaces in ultra-thin epitaxial V/Gd bilayers

L. T. Baczewski,* P. Pankowski, and A. Wawro

Institute of Physics, Polish Academy of Sciences, Al. Lotnikow, 32/46, Warsaw, Poland

K. Mergia and S. Messoloras

*Institute of Nuclear Technology & Radiation Protection, National Centre for Scientific Research "Demokritos,"
15310 Aghia Paraskevi Attikis, Greece*

F. Ott

Laboratoire Léon Brillouin, CEA-Saclay, 91191 Gif-sur-Yvette Cedex, France

(Received 9 March 2006; revised manuscript received 24 May 2006; published 16 August 2006)

The magnetic structure of epitaxial vanadium/gadolinium bilayers with different V thickness has been studied using polarized neutron reflectivity and magnetization measurements. The polarized neutron reflectivity results show that in the fully magnetized state of V/Gd bilayer about three to five monolayers of V become magnetic with a mean magnetic moment of around $0.8 \mu_B/\text{atom}$. The V slab is antiferromagnetically aligned with the Gd layer. From magnetization measurements it has been found that the Curie temperature of the V/Gd system is increased by 74 K in comparison to that of a Gd layer without vanadium.

DOI: [10.1103/PhysRevB.74.075417](https://doi.org/10.1103/PhysRevB.74.075417)

PACS number(s): 75.70.-i, 75.70.Cn, 75.25.+z

I. INTRODUCTION

Induced magnetism in thin films has recently been intensively studied due to the developments in deposition techniques as molecular beam epitaxy (MBE) and the availability of experimental techniques probing magnetic properties with element specificity combined with monolayer (ML) sensitivity such as x-ray magnetic circular dichroism (XMCD), x-ray magnetic scattering, and polarized neutron reflectivity (PNR). Layered structures composed of ferromagnetic and nonmagnetic metals are interesting for both technological applications and fundamental research. Most of the studies have been carried out in layered systems consisting of magnetic $3d$ and nonmagnetic $3d$ or $5d$ transition metals and mainly as a $3d$ metal iron or nickel has been used. Interfacially induced magnetic moments of the $5d$ elements such as Pt, Ir, W in multilayers with Ni and Fe have been reported.^{1,2} Ferromagnetic coupling was found for Pt and Ir while W was antiferromagnetically coupled to Ni and Fe. XMCD results showed an induced magnetic moment of $0.17\text{--}0.29 \mu_B/\text{at}$ for Pt and $0.2 \mu_B/\text{at}$ for W and Ir at the interface decaying rapidly inside the layer. On the contrary in Gd/W multilayers no measurable spin polarization in W was detected by PNR.^{3,4}

The most extensively studied system consisting of magnetic $3d$ —nonmagnetic $3d$ transition metal is the Fe/V system and a number of different techniques as SQUID, CEMS, or PNR (Refs. 5–7) have been used. Results of recent theoretical and experimental papers concerning Fe/V (Refs. 8–13) clearly show an induced magnetic moment in V, which is antiferromagnetically coupled to the Fe moments of the neighboring layers. However, there is a disagreement concerning the range of polarization in V between theory and experiment. Theoretical papers^{14–16} for the Fe/V system show a strong but short range magnetic polarization in vanadium, where magnetic moments are localized mostly at the interface vanadium atoms. FP-LMTO calculations¹⁴ predict an induced vanadium magnetic moment of $0.93 \mu_B/\text{atom}$

only for the interface atoms with a simultaneous reduction of the Fe magnetic moment in the vicinity of vanadium. However, from XMCD measurements on the Fe/V system^{17,18} it was found that the induced magnetic moment in V is extended up to 4 monolayers from the Fe/V interface. In recent XMCD measurements performed at $L_{2,3}$ edges of Fe and V for Fe/V/Fe trilayers^{2,19} a short range polarization was concluded from the signal saturation above 3 ML of V.

The experimentally determined values of V induced moments differ considerably between a Fe/V/Fe trilayer and an epitaxial Fe/V multilayer. For the trilayer² a V magnetic moment of $0.5 \mu_B/\text{at}$ was determined but a moment of $0.9 \mu_B/\text{at}$ for Fe/V multilayer¹⁰ has been reported. This difference can be explained taking into account theoretical *ab initio* calculations carried out by Coehoorn¹⁶ showing that an induced magnetic moment of V atom depends on the number of the Fe nearest neighbors in its vicinity, which is closely related to the interdiffusion at the interfaces. The influence of the interface roughness and interdiffusion processes on the enhancement of V polarization has clearly been shown in the case of Fe/V/Fe trilayers deposited at different temperatures.²⁰ The magnitude of the induced V moment is increased by a factor of two upon changing the deposition temperature from 300 K to 600 K.

The magnetic behavior of Gd-TM alloys is ruled by the antiferromagnetic exchange interactions between a heavy rare-earth (Gd) and a transition metal (Fe, Co). This antiparallel coupling between RE-TM is a matter of interest, especially in multilayers, where a variety of spin configurations appear because of the balance between exchange and Zeeman terms.²¹ Gd, Fe, and Co are all ferromagnetic in the bulk, but the magnetic coupling across the Fe/Gd or Co/Gd interface is antiferromagnetic.^{22–27} Under special deposition conditions where the RKKY (interlayer) exchange interaction dominates the direct exchange ferromagnetic state can be realized in TM/Gd systems.²⁸ Another interesting example is the Gd/Y superlattices. Although Y is nonmagnetic, there is an effective antiferromagnetic interaction between blocks

TABLE I. Structural parameters determined by x-ray and neutron reflectivity data. Numbers inside parenthesis are the roughness values.

Sample	Temperature (K)	Radiation	Thickness (nm)				
			Mo	V	Gd	GdAl	Al
Gd reference	5	PNR	19.7 (0.26)	—	2.9 (1.0)	4.3 (2.3)	15.3 (1.54)
V(4ML)/Gd	300	X-ray	23.7 (0.13)	1.23 (0.56)	4.2 (1.2)	5.5 (0.72)	11.8 (2.11)
		PNR	23.6 (0.15)	1.27 (0.5)	4.1 (1.24)	5.9 (0.89)	11.7 (2.12)

of Gd spins for certain thickness of intervening Y layers.²⁹ Vanadium in the bulk is nonmagnetic, however, as it has been mentioned above, at interfaces where there is lower coordination number and lattice expansion it can acquire a large magnetic moment and generally aligns antiferromagnetically with TM (e.g., Fe/V). The electronic structure is quite different between TM and RE. The rare-earth metals are strongly correlated materials. The open shell of highly localized $4f$ electrons is responsible for their large magnetic moments. The overlap with the $4f$ shells on neighboring lattice sites is negligible. Therefore, the $6s$, $6p$, and $5d$ states play an essential role in the magnetism, because they mediate the magnetic interaction by a Ruderman-Kittel-Kasuya-Yosida-(RKKY-) type exchange, although their contribution to the magnetic moment is small.

Thus, it would be interesting to examine the V/Gd interface magnetic structure to determine if V acquires a magnetic moment in such bilayer and if, as for the transition metals such as Fe and Co, it aligns antiferromagnetically with Gd.

II. EXPERIMENTAL DETAILS

The ultra-thin epitaxial V/Gd bilayers were grown using MBE technique at a vacuum level of the order of 10^{-10} Torr. In order to achieve epitaxial growth a sapphire substrate with orientation (11-20) and a Mo buffer layer of about 20 nm were used. The Al_2O_3 substrate was chemically cleaned and degassed in vacuum at high temperature in order to avoid contamination. The V layer was grown on the Mo(110) buffer. Samples with V nominal thickness of 4, 8, 10, and 11 monolayers were grown. Also a reference sample without V (Table I) was fabricated. Directly on the V layer a Gd film of nominal thickness of about 6 nm (20 ML) was deposited. An Al cover layer of 10 nm was used for protection against oxidation (Initially Y was used as a protective layer but a significant reduction of magnetization occurred after one month showing that Y could not be used as a cap layer for the reactive Gd. Consequently Al was used as a protective layer, which is known to produce a compact oxide layer on the surface). All the materials were evaporated from electron guns. Deposition rate during growth process was kept at a level of 0.5 \AA/s and was controlled by the electron impact emission spectroscopy (EIES) based Sentinel III system. The Mo buffer layer was deposited at the temperature above

1000 °C in order to obtain optimal crystalline structure and minimum surface roughness. The V layers deposition process was performed at 700 °C and the Gd was deposited at room temperature. The resulting sample structure was $\text{Al}_2\text{O}_3/\text{Mo}/\text{V}/\text{Gd}/\text{Al}$. The quality of the interfaces and the crystallographic orientation were investigated *in situ* by 12 kV reflected high energy electron diffraction (RHEED). Auger spectroscopy (AES) was carried out also *in situ* and no surface contamination of the deposited metallic layers was observed.

Hysteresis loops were measured at 5 K and in an external magnetic field up to 2 T applied in the film plane using a vibrating sample magnetometer (VSM). Coercive field values are in the range from 0.044 to 0.052 Tesla. The rectangular shapes of measured hysteresis loops with high remanence show in-plane anisotropy for all the samples (M_r/M_s close to 1).

The x-ray reflectivity measurements using synchrotron radiation (this was necessary due to the limited thickness of the bilayers) were performed at room temperature at the W 1.1 station at HASYLAB in Hamburg at a wavelength of 0.124 nm and the employed Q range was from 1.15 to $3.5 \times 10^{-2} \text{ nm}^{-1}$. The PNR measurements were carried out on the PRISM instrument at Laboratoire Léon-Brillouin, CEA-Saclay, at 5 K and with an in-plane external magnetic field of 1.5 T in order to magnetically saturate the samples. The wavelength used was 0.43 nm and the Q range was from 0.05 to 0.7 nm^{-1} . The spin-up and spin-down reflectivities (R^+ , R^-) of the reference sample and the four V/Gd samples were measured. The data have been corrected for the polarization efficiency. The least squares fitting of all the reflectivity data (x rays and neutrons) was made using the Simul-Reflec software.³⁰ For the scattering lengths of x rays and neutrons and absorption cross sections the tabulated values were employed.

III. EXPERIMENTAL RESULTS AND ANALYSIS

At first the structure of the V/Gd bilayers is discussed as it has a strong influence on their magnetic properties. Next in order to determine the magnetic structure and behavior of Gd thin film, the results for the reference sample (without V layer) are presented. Finally the magnetic behavior of the V in V/Gd bilayers is analyzed.

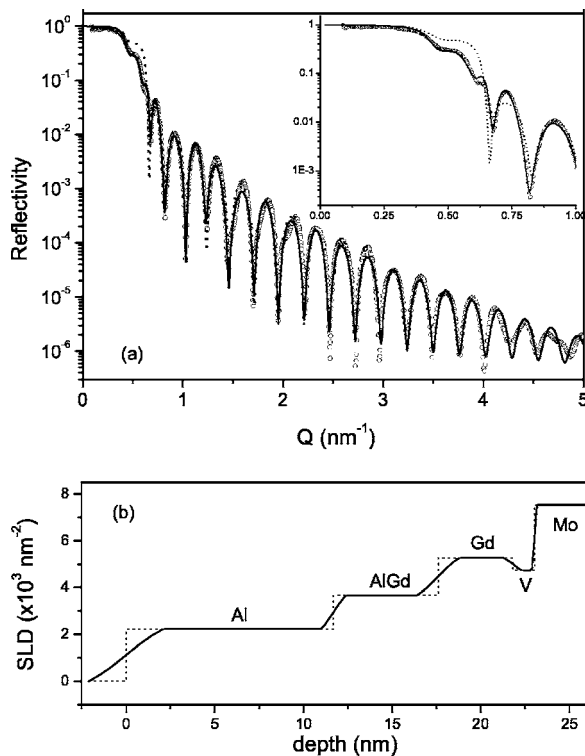


FIG. 1. (a) x-ray reflectivity curve and the least squares fitted models for the V(4 ML)/Gd sample. Open circles represent experimental data. Dotted line: model without a AlGd layer (no Gd and Al intermixing). Solid line: model with a AlGd layer (Gd and Al intermixing). (b) Scattering length density (SLD) versus depth profile [see Eqs. (A9) and (A10)]. Dotted lines indicate sharp interfaces

A. Structural characterization of the V/Gd bilayers

RHEED *in situ* observations performed in sequence during thin films growth showed that the spacing of 20 nm thick buffer Mo between (110) planes was equal to that of the bulk. The following relations between in-plane directions of the constituent layers were found: Mo(110)/V(110):[001]||[001], V(110)/Gd(0001):[001]||[11-20]. These epitaxial relationships of V/Gd correspond to the Nishiyama-Wasserman orientation. The epitaxial Gd growth on Mo(110) (in the reference sample) and on V(110) (in the Gd/V samples) was identical conserving the Nishiyama-Wasserman relations, resulting in Gd(0001) orientation and two-dimensional (2D) growth mode, which was confirmed by sharp streaks in RHEED images for both cases.

The structure of the V/Gd bilayers and that of the reference Gd sample was determined by synchrotron x-ray reflectivity measurements. Interpretation details of the x-ray reflectivity measurements have been discussed elsewhere.³¹ Here we mention that two models have been used to explain the observed x-ray reflectivity curves. In the first model it is assumed that there is no intermixing between Al cover layer and Gd, whereas in the second model an intermixing is incorporated. The experimental x-ray data together with curves for both fitted models for the V(4 ML)/Gd sample are presented in Fig. 1(a). It is apparent that the model assuming that there is an intermixing of Al and Gd gives a much better

fit to the experimental data. The AlGd mixed layer has a chemical formula of $\text{Al}_{0.6}\text{Gd}_{0.4}$ as it was found by the least squares fit and this value was obtained for all the studied V/Gd bilayers. The intermixing of Al and Gd is not surprising since the formation enthalpy of Al-Gd alloys at room temperature is the lowest at around $\text{Al}_{0.58}\text{Gd}_{0.42}$ and negative for a whole range of other compositions.³² The density of the rest of the layers (Mo, V, Gd, Al) in all the samples was found to be very close to that of the respective bulk value. Also the roughness [see Eqs. (A9) and (A10)] of the layers was determined from the x-ray reflectivity. Given that an extended Q range for the x-ray reflectivity measurements was employed the structural layer parameters were determined quite accurately and for example the vanadium layer roughness in the V(4 ML)/Gd sample determined from the x-ray data is consistent with AFM measurements of a layer of similar thickness.³³ In Table I the structural parameters of the V(4 ML)/Gd sample are given and its scattering length density (SLD) is presented in Fig. 1(b). The gradual (no abrupt) change of the SLD at the interfaces is due to roughness of the layer. With the term roughness is meant that the interface is not flat and the presented SLD versus depth profile is its xy plane average [see Eq. (A9) in the Appendix].

In Fig. 2(a) the spin-up and spin-down polarized neutron reflectivities of the V(4 ML)/Gd sample at 300 K (above T_c for Gd) are presented. We observe that there is no splitting between the spin up and spin down reflectivities, which shows that the sample is not magnetic. Thus, this measurement can be used for the determination of the structural parameters of the sample independently of the x-ray reflectivity measurements. The thickness of the layers derived from PNR agree with those derived from x-ray reflectivity with an accuracy better than 3% (see Table I).

It can be seen from Table I that the roughness of the V layer is considerable relative to its thickness and it might be interpreted as an indication of V and Gd intermixing. However, such an intermixing can be excluded on the following reasons (a) binary alloy phase diagram of Gd-V system shows that both elements are immiscible, (b) the Gd was deposited at room temperature and its epitaxial growth was observed by RHEED, and (c) no intermixing of Gd and V even in film structures and at temperatures as high as 700 °C has been observed earlier.^{34,35} Furthermore, the reflectivity experiments are very sensitive in determining any intermixing, if it had occurred for any reason after the preparation of the samples.

In the insert in Fig. 2(a) the relative reflectivity difference (RRD) [$\text{RRD} = (R_{\text{fitted}} - R_{\text{model}}) / R_{\text{fitted}}$, where R_{fitted} is the least squares fitted reflectivity and R_{model} —the reflectivity calculated for a specific model] for models assuming different degrees of V-Gd intermixing is presented. From the insert it is observed that any intermixing has to be less than 2% of Gd atoms in the vanadium layer.

Thus, in summary, similar quality of Gd(0001) layer has been grown either on Mo (in the reference sample) or on V (in the V/Gd bilayers) and the further deposition of Al on Gd results in a development of AlGd alloy layer. In all the V/Gd bilayers a pure Gd layer of thickness larger than 3 nm remains with a density very close to that of the bulk. The thickness of the constituent layers, their densities and inter-

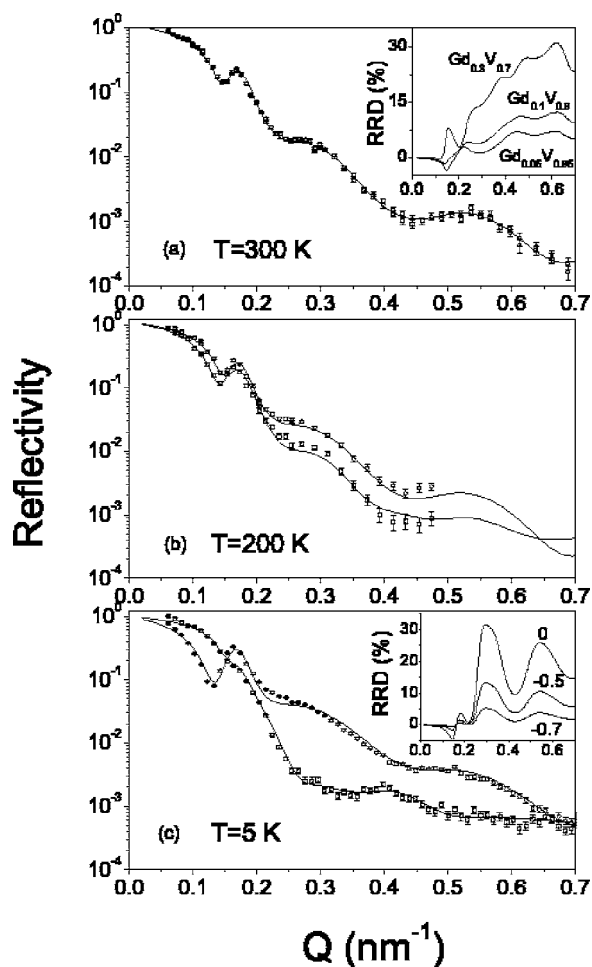


FIG. 2. PNR data for the V(4 ML)/Gd sample at different temperatures. Experimental data: \square for R^+ (spin up) and \circ for R^- (spin down). Solid line: Least squares model fitting. Inset (a): the relative reflectivity difference (RRD) between the least squares fitted model and models assuming different degrees of V-Gd intermixing. Inset (c): RRD for models assuming different V magnetic moments.

facial roughness have been determined by x-ray reflectivity measurements and were confirmed independently by PNR experiments at 300 K. Furthermore, the reflectivity data exclude any intermixing of the V and Gd.

B. Magnetic structure of the reference sample

Since Gd as a thin film might have different magnetic behavior and/or moment than in the bulk, its magnetic state has to be analyzed first. For this PNR and magnetization measurements of the reference sample (i.e., a sample having the same structure and growth conditions as the V/Gd bilayers but without V layer) were performed.

The PNR spin up (R^+) and spin down (R^-) reflectivities of the reference sample (Fig. 3) were fitted for both models i.e., without or with intermixing between the Gd and Al. From Fig. 3 it is apparent that the model assuming no intermixing of Gd and Al fails to reproduce the experimental data. This failure is more apparent in PNR than in the x-ray reflectivity

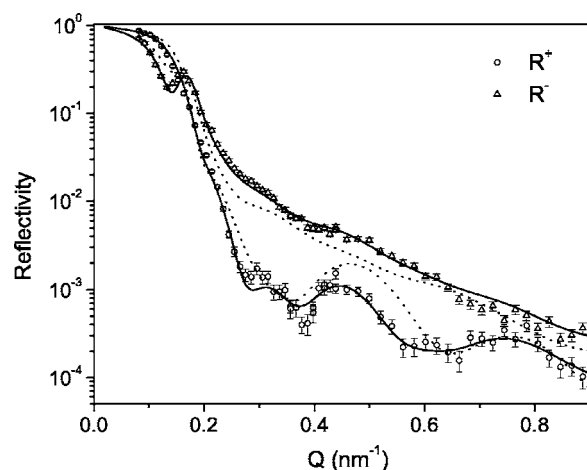


FIG. 3. PNR data for the reference sample at 5 K. Experimental data: \circ for R^+ and \triangle for R^- . Dotted line: Model without an AlGd layer (no Gd and Al intermixing). Solid line: Model with an AlGd layer (Gd and Al intermixing).

data as the contrast between Gd and Al for the neutrons (nuclear plus magnetic) is higher than that for the x rays. The magnetic moment of the AlGd mixed layer was found to be $0.32 \mu_B/\text{atom}$ and the Gd moment $7.1 \pm 0.2 \mu_B/\text{atom}$ (Gd bulk value is $7.63 \mu_B/\text{atom}$). The chemical composition of the AlGd layer was found to be around $\text{Al}_{0.6}\text{Gd}_{0.4}$, which agrees extremely well with the chemical composition, determined from the x-ray reflectivity measurements for the V/Gd bilayers (see Sec. III A). Thus, not only the crystallographic structure of the Gd layer is very close to that of the bulk (Sec. III A) but also its magnetic moment. The magnetic moment per atom versus depth profile of the reference sample is presented in Fig. 4(a).

It is well known that the Curie temperature of Gd thin films decreases as the film thickness is reduced. This is also true for the Gd film of the reference sample, as it can be seen in Fig. 5, where the magnetization versus temperature dependence is presented. The AlGd contribution to the total sample magnetization is around 6% and it can, thus, be ignored. From the shape of magnetization versus temperature curve we can construe, using the mean field theory, that there are two molecular field distributions (α and β) giving rise to two transition temperature ranges and the smooth appearance of the curve. Other investigators have found a similar magnetization versus temperature behavior in thin film Gd structures.³⁶ The experimental data have been fitted using Eq. (A7) (see the Appendix) and the derived parameters are presented in the legend of Fig. 5. The mean transition temperatures corresponding to the two molecular field distributions α and β are $\langle T_c^\alpha \rangle = 77 \text{ K}$ and $\langle T_c^\beta \rangle = 168 \text{ K}$, respectively.

Since the magnetization data predominantly reflect the magnetization of the Gd layer, the two molecular field distributions (α and β) have to be correlated with the Gd magnetic moment versus depth profile determined by PNR and shown in Fig. 4(a). It is apparent that the lower transition temperature has to be attributed to the Gd atoms at the AlGd/Gd interface or near it, whereas the higher transition temperature to the unperturbed Gd layer. In the Appendix is shown how from the saturation magnetization of the two molecular field

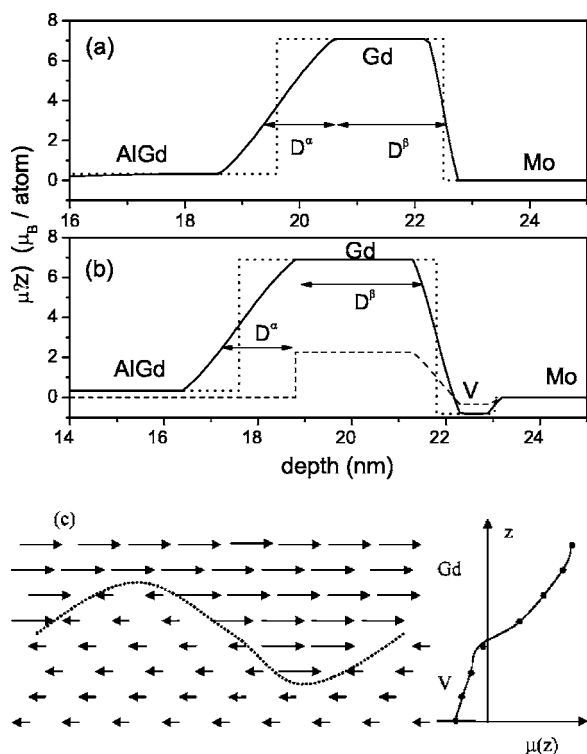


FIG. 4. Magnetic moment vs depth profile for (a) reference sample and (b) for V(4 ML)/Gd sample. Dotted lines indicate hypothetical sharp interfaces. Continuous line: indicates the magnetization profile at 5 K, dashed line: magnetization profile at 200 K. Arrows show the regions corresponding to the two molecular field distributions α (D^α) and β (D^β). (c) Magnetic structure schematic representation of V-Gd interface—indicating the meaning of the magnetic moment versus depth profile shown in (a) and (b).

distributions (μ_s^α and μ_s^β , see legend of Fig. 5) we can calculate the corresponding regions (D^α and D^β) of the Gd layer. These two regions are shown in Fig. 4 with arrows. We observe that region α , having the lower transition temperature, corresponds to Gd atoms at the interface and region β , having the higher transition temperature, to the unperturbed part of the Gd layer.

C. Magnetic structure of the V/Gd bilayers

At first we will discuss the magnetization versus temperature measurements of the V/Gd bilayers. VSM magnetization measurements of these samples predominantly reflect the magnetization of the Gd layer since any possible contribution of the V to the total magnetization is very small (Even if we assume the magnetic moment of V as $1 \mu_B/\text{atom}$ the contribution of V to the total magnetization would be only 4%.) Whereas, it is impossible to deduce any magnetic moment of V from magnetization measurements, these experiments are essential in order to investigate if any magnetic change has been induced in the Gd by the adjacent vanadium layer. The magnetization versus temperature curve of the V(4 ML)/Gd bilayer is presented in Fig. 5. Although the shape of the magnetization curve of V(4 ML)/Gd bilayer is very similar to that of the reference sample, it is apparent that the

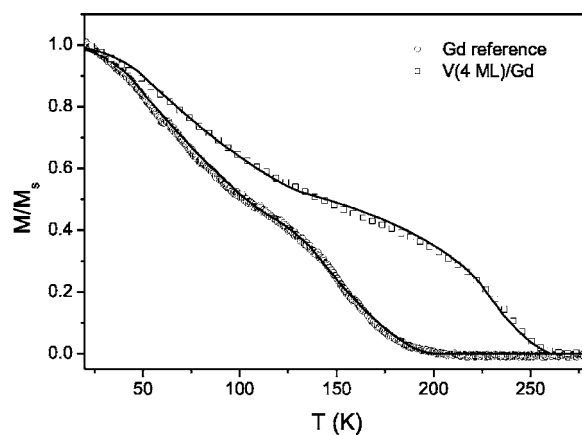


FIG. 5. Magnetization vs temperature dependence (at $H=300$ Oe). \circ : experimental data for the reference sample, solid line: least squares fit (see the Appendix). Least squares determined parameters: $\mu_s^\alpha=0.38$, $T_{c1}^\alpha=45$ K, $T_{c2}^\alpha=110$ K, and $\mu_s^\beta=0.62$, $T_{c1}^\beta=140$ K, $T_{c2}^\beta=197$ K. \square : experimental data for the V(4 ML)/Gd, solid line: least squares fit (see the Appendix). Least squares determined parameters: $\mu_s^\alpha=0.38$, $T_{c1}^\alpha=50$ K, $T_{c2}^\alpha=130$ K, and $\mu_s^\beta=0.62$, $T_{c1}^\beta=225$ K, $T_{c2}^\beta=260$ K.

presence of 4 ML of V has resulted in a significant increase of the transition temperature of the Gd layer. This must be arising from a magnetic interaction between the vanadium and gadolinium, which consequently means that the V has acquired a magnetic moment. This is corroborated by the fact that all four studied V/Gd bilayers have very similar $M(T)$ curves with very close transition temperatures. Since the transition temperature increase is independent on the V layer thickness, we can infer that only a part of the V layer (at the interface or near it) has become magnetic.

The mean field approach employed for the interpretation of the $M(T)$ curve of the reference sample (see Sec. III B) has also been applied to the magnetization data of the V/Gd bilayers. In Fig. 5 we observe an excellent agreement between the experimental data for the V(4 ML)/Gd sample and the least squares fitted curve (the parameters obtained from the least squares fit are given in the legend of Fig. 5). The saturation magnetization of the two molecular field distributions in the V(4 ML)/Gd sample are equal to those of the reference sample showing that the magnetic structure of the Gd layer in both samples is quite similar. However, the lower mean transition temperature has been increased from 77 K in the reference sample to 90 K in the V(4 ML)/Gd sample and the higher mean transition temperature from 168 to 242 K.

Before we proceed to discuss the PNR data we summarize the experimental findings discussed above as: (a) the crystallographic structure of Gd layers in all samples is the same, (b) the magnetic structure of the Gd layers in all samples is quite similar, and (c) the V layer has increased the transition temperature of the Gd layer by 74 K [see $M(T)$ measurements].

Since the magnetization versus temperature measurements have shown that a Gd-V magnetic interaction is present, the purpose of the PNR measurements has been the determination of the V atoms magnetic moment value. It would have been arguable if PNR measurements could be

adequate in determining an expected small magnetic moment of V in the presence of a large Gd moment. For this reason the number of parameters to be determined by PNR had to be minimized and additional experimental information had to be provided in order to unambiguously determine the V moment. In order to minimize the parameters to be fitted to the PNR curves the structural parameters of the samples have been determined by x-ray reflectivity and it has been established above that the x-ray derived structural parameters are in agreement with those obtained by PNR measurements carried out when the sample is not magnetic. In addition PNR measurements were carried out also at 200 K. At this temperature, as it has been found out by $M(T)$ measurements (see Fig. 5), the reference sample is not magnetic, whereas the V/Gd bilayers are magnetic. From the $M(T)$ curve we can predict the reduction of Gd magnetic moment in comparison to its value at 5 K and such a reduction has to be also observed in the PNR measurements. As the V is responsible for the increase of the Gd transition temperature, it should also be expected to be magnetic at 200 K and its magnetic moment to be reduced from its value at 5 K in a similar manner as the Gd magnetic moment. A further constraint is introduced by measuring the PNR for the four V/Gd samples with different V thickness. It is expected that the V atomic moment (in μ_B/atom) in all studied V/Gd samples would either remain constant or to be reduced with increasing V thickness. The latter behavior is more in accordance with the magnetization measurements, which hint that only a top slab of the vanadium close to interface with Gd is magnetically active. Thus, in order to prove unambiguously the existence of V induced moment at Gd/V interface all the above listed relations and results must be confirmed and consistent.

The experimental PNR data for the V(4ML)/Gd sample at 5 K are presented in Fig. 2(c) together with the least squares fitted curves. From the fitting it has been found that the magnetic moment of the Gd is $6.9 \mu_B/\text{atom}$, a value very close to that derived for the reference sample ($7.1 \mu_B/\text{atom}$). As it has been discussed above, since the crystallographic and magnetic structure of the Gd in V/Gd layers and the reference sample are very alike, close values of the Gd atomic magnetic moments are expected. It was also found that vanadium has an induced atomic magnetic moment of $-0.8 \mu_B/\text{atom}$ and it is antiferromagnetically coupled to the Gd layer. In the insert of Fig. 2(c) the normalized difference of the spin up reflectivity to that of the least squares fitted curve is presented for different V moments. These curves show the Q range, which is mostly sensitive to the V magnetic moment. The figure also shows the way the least squares fit converges from V starting magnetic moment of zero. In order to verify that a global minimum of the χ square parameter was attained least squares fits were performed with different starting pairs of Gd and V moments and always the final values were within less than 1% difference from the quoted magnetic moment values. In order to ascertain the magnetic moment values and their errors, a series of reflectivity curves were calculated using different pairs of V and Gd moments. The pairs, which gave reflectivity curves obviously deviating from the data, were taken as to define the limits of accuracy and all these pairs are included within 5% of the quoted magnetic moment values.

In Fig. 4(b) the magnetic moment versus depth profile of the V(4 ML)/Gd sample is presented where a continuous line indicates magnetization profile at 5 K, and a dashed line -: magnetization profile at 200 K. It should be noted that no sharp interface represents the roughness of the layer. As it is described in the Appendix the magnetic moment versus depth is the xy plane average of the magnetic moment and not a magnetic moment of an alloy (in Sec. III A it has been proved that there is no V-Gd alloying). A schematic of the V-Gd interface is presented in Fig. 4(c) as well as the meaning of the xy plane averaging of the magnetic moment, as an interface region is cross sectioned. The regions of the Gd layer (D^α and D^β) corresponding to the two molecular field distributions are also shown (see Sec. III B and the Appendix). From Fig. 4 we observe that the magnetic structure and moment of the Gd layers in both the reference and the V(4 ML)/Gd samples are very close. However, the transition temperature of the region β of the Gd layer adjacent to the V layer in the V(4 ML)/Gd sample has increased by 74 K in comparison to the reference sample, whereas the transition temperature of region α (at AlGd/Gd interface) by only 13 K.

In Fig. 2(b) the PNR data of the V(4 ML)/Gd bilayer at 200 K are presented. From the spin up and spin down splitting of the reflectivity curves [for comparison see Fig. 2(a)] we conclude that this sample is magnetic, contrary to the reference sample (see Fig. 5). From the magnetization data we have found that the transition temperature for region α is 90 K, thus this region is not magnetic at 200 K and this has been incorporated in the fitting of the reflectivity curve. From the least squares fitting it was found that the Gd and V magnetic moments have been reduced from their values at 5 K to $2.24 \mu_B/\text{atom}$ and $-0.34 \mu_B/\text{atom}$, respectively. It means that we observe a 32% reduction of the Gd magnetic moment from its value at 5 K and simultaneously a 31% reduction of the V magnetic moment. Thus, the temperature increase from 5 to 200 K results in an almost equal reduction of both V and Gd moments. This reduction of the magnetic moments is in accordance with the $M(T)$ curve (Fig. 5) where the magnetization at 200 K has been reduced to 38% of its value at 5 K. Thus, the prerequisites set above for consistency of the PNR and magnetization data, i.e., similar reduction of V and Gd magnetic moments have been fully satisfied.

The PNR data of the rest of V/Gd samples were analyzed in the same way as those of V(4 ML)/Gd and the least squares deduced respective magnetic moments of the V and Gd atoms are presented in Table II. We observe that the V magnetic moment per atom is reduced as the V layer thickness is increased. The $M(T)$ curves for the rest of the V/Gd samples are quite close to that of the V(4 ML)/Gd bilayer, thus the analysis and the results obtained for the V(4 ML)/Gd hold for all the V/Gd bilayers. In the last column of Table II the product of the V atomic magnetic moment multiplied by its layer thickness is calculated ($d\mu$). One can observe that this value is almost constant for all V/Gd bilayer samples (maximum deviation from the mean value is around 4%), which demonstrates the consistency and accuracy of the V magnetic moments derived from PNR. From the mean value of this product $\langle d\mu \rangle = (4.5 \pm 0.3) \text{ ML} \times \mu_B$ assuming that the

TABLE II. Thickness and magnetic moments of V and Gd layers. Layer thickness d and roughness (numbers inside parenthesis) were determined by x-ray reflectivity. Magnetic moments $\langle\mu\rangle$, determined by PNR, μ is magnetic moment of unperturbed Gd [see Fig. 4(b)].

Sample	Temp. (K)	Gd			V		
		d (nm)	$\langle\mu\rangle$ (μ_B/atom)	μ	d (nm)	$\langle\mu\rangle$ [μ_B/atom]	$\mu \times d$ [$\mu_B \times \text{ML}$]
Gd reference	5	2.9 (1.0)	7.1	7.4	—	—	—
V(4ML)/Gd	200	4.2 (1.2)	2.2	—	1.23 (0.56)	-0.34	—
	5	4.2 (1.2)	6.9	7.5	1.23 (0.56)	-0.82	4.7
V(8ML)/Gd	5	3.8 (0.8)	6.7	7.1	2.03 (0.15)	-0.48	4.6
V(10ML)/Gd	5	3.4 (0.6)	6.5	6.9	2.45 (0.5)	-0.35	4.0
V(11ML)/Gd	5	2.7 (1.2)	6.3	7.3	3.11 (0.7)	-0.36	5.2
				7.2 ± 0.2 a			4.6 ± 0.5 a

^aMean value and standard deviation of the numbers in the column.

whole V layer in the sample with the thinnest V layer is magnetically active (5.6 ML) we obtain a magnetic moment of the vanadium $-(0.80 \pm 0.05) \mu_B/\text{atom}$. It is apparent that if we assume thinner V magnetically active slab the larger V magnetic moment will be obtained and thus the value of $-0.8 \mu_B/\text{atom}$ is a lower limit of the V moment.

From Table II we observe that the Gd moments, $\langle\mu\rangle$, for the four V/Gd samples are the same within the quoted error of 10% (see above). It should be reminded that the magnetic moments determined from the PNR data are mean values, which are taken over the whole layer volume. The Gd layer does not have a sharp interface but there is a magnetization profile as that shown in Fig. 4(b). Using the same procedure as that used for the reference sample (Sec. III B) the Gd magnetization profile for the studied V/Gd samples has been calculated and the Gd moment at the V interface is presented in Table II as (μ). From Table II we observe that Gd magnetic moments are very close and almost equal to the bulk value of Gd moment for all the samples. In order to exclude any possibility that the V has induced a magnetic moment to the Mo layer, a 1 nm thick V layer was deposited on Mo(110) buffer at the same growth conditions and SQUID $M(H)$ measurements have not shown any magnetization. Finally the PNR derived Gd and V magnetic moments have been used to calculate the bulk saturation magnetization of the V/Gd samples. A very good agreement between the saturation magnetization calculated from the microscopically derived parameters from PNR and the macroscopic VSM measurements has been found.

In concluding the presented above analysis it should be noted that all the constraints set for the interconsistency of the derived parameters have been fulfilled so the conclusion about the existence of an induced V magnetic moment in Gd/V bilayers is justified.

IV. DISCUSSION

The purpose of this study has been to investigate the V/Gd interface magnetic structure, i.e., to determine if the V acquires magnetic moment in the vicinity of Gd and its magnetic coupling direction with the Gd. In order to ascertain whether there is a surface or bulk magnetization state of V, samples with different V thickness were fabricated by MBE (Table II). The crystallographic structure of the layers was monitored *in situ* by RHEED, which showed that the in-plane directions relation V(110)/Gd(0001) was satisfied for every sample. The thickness, density and roughness of the constituent layers in the studied samples were determined by x-ray reflectivity measurements and the PNR measurements were used for the determination of the magnetic moments.

From the PNR data of four V/Gd samples the V and Gd magnetic moments have been determined (see Table II). In all the V/Gd bilayers it has been found that a magnetic moment has been induced in the V and that the V layer is antiferromagnetically coupled to the Gd layer. The product of the vanadium layer thickness by its moment is almost constant for all studied V/Gd samples, which demonstrates that only a top slab of vanadium layer close to the interface with Gd is magnetically active. The thickness of this slab is less or equal to 5 ML and the induced vanadium magnetic moment higher or equal to $0.8 \mu_B/\text{atom}$ (thinner magnetically active slabs imply larger V moments).

The V ground state and its magnetic moment strongly depends on the atomic distance,³⁷ number and type of neighbors^{38,39} and for V slabs or layers antiferromagnetic structures occur for exchange integral values smaller than those for ferromagnetic structures.⁴⁰ In this work we have found that the vanadium atoms at the interface with Gd have acquired a magnetic moment and this interface as it has been found by AFM and x-ray reflectivity measurements is quite

rough. Thus, it could be deduced that the roughness is further reducing the number of V next neighbors, distorts the bond lengths and angles and between 3 to 5 monolayers of V acquire a magnetic moment. Also, the lattice strain occurring at the interfaces during epitaxial growth of hcp Gd on bcc metal has been theoretically suggested to be a cause of antiferromagnetic ordering at the interface.⁴¹ Large magnetic moments for V have been already reported for Fe/V (Refs. 18 and 10) and Co/V systems.⁴² We have found that the V-Gd coupling is antiferromagnetic, the V-V coupling and the Gd-Gd coupling is ferromagnetic with Gd atoms having a magnetic moment close to the bulk value. Thus, we observe a similar situation as that reported for Fe/V multilayers where the V atoms within a slab of 3 ML, a value close to our findings, are magnetic and antiferromagnetically coupled to the Fe layer. Recently a published paper on Mössbauer spectroscopy in Gd/Cr multilayers⁴³ also supports our findings. The authors reported a significant increase of hyperfine field HF on Cr nuclei at 5 K induced by the presence of Gd films. As Cr and V are both 3d transition metals the same mechanism is possible in these two cases.

Magnetic properties of Gd in TM/RE systems are determined by its *d* electrons, since the coupling of the 4*f* local moments below the ordering temperature is solely determined by the dominant 4*f*-5*d* exchange interaction.⁴⁴ Hybridization of the 3*d*-5*d* via the 5*d*-4*f* exchange couples the Gd 4*f* local moments antiparallel to the V moments. This indirect coupling has also been observed in the system of Gd/Co.⁴⁵ The V-V moments are coupled ferromagnetically through direct 3*d*-3*d* interactions.

The Gd-V coupling is manifested in the magnetization versus temperature measurements and PNR results at 200 K. From the PNR measurements at 200 K it has been found that both the magnetic moments of Gd and V atoms have been reduced of about 30% in comparison to their corresponding values at 5 K. This shows that the V-Gd magnetic coupling remains up to this temperature, at which a Gd layer in the reference sample without V is not magnetic. From the $M(T)$ curves it has also been found that the transition temperature has been increased by about 74 K for all four studied V/Gd samples in comparison to the reference sample, i.e., it is independent on either V or Gd thickness. Thus, the effect observed here is not due to the dependence of the Curie temperature on the Gd film thickness (Refs. 46 and 47) but it is connected with the V-Gd magnetic coupling. Thus, the Curie temperature increase has to be attributed to the strength of the 3*d*-5*d* V and Gd coupling and such a strong coupling has also been found in the antiferromagnetically coupled Gd/Fe system, where a Gd monolayer attains a Curie temperature at 800 K.⁴⁸

V. CONCLUSIONS

High quality MBE grown epitaxial bilayers of V/Gd have been fabricated with the V layer thickness varying from 4 to 11 ML. The epitaxial relationships of V/Gd correspond to the Nishiyama-Wasserman orientation. The structural parameters of the bilayers have been determined by synchrotron x-ray reflectivity measurements and their magnetic

structure—by polarized neutron reflectivity (PNR) and VSM magnetization measurements.

The main conclusions are the following:

(i) The V has acquired an induced magnetic moment at the interface with Gd. This is proven by the magnetization versus temperature measurements showing that the Curie temperature of the V/Gd bilayers has been increased by 74 K when compared to the reference sample (sample with the same structure but without a V layer).

(ii) The magnetic moments of Gd and V have been derived by PNR measurements at 5 K. The mean magnetic moment of the Gd atoms are close to that of the bulk. The V mean magnetic moment is found to be decreasing with V layer thickness, which shows that only a top slab of maximum 5 ML of the V layer at the V/Gd interface is magnetically active. The mean magnetic moment of the V atoms is about $-0.8 \mu_B/\text{atom}$.

(iii) The V-Gd antiferromagnetic coupling remains at higher temperatures as it is shown by PNR measurements at 200 K, where the same reduction of the Gd and V moments in comparison to their values at 5 K was found. This is in full agreement with the $M(T)$ results.

(iv) The V induced moment is an interface effect and is probably arising from a change of the type and number of neighbors. The Gd 4*f* local moments are coupled antiferromagnetically to the V moments through a hybridization of the 3*d*-5*d* electron orbitals via the 5*d*-4*f* exchange. The V-V coupling is ferromagnetic through direct interactions.

ACKNOWLEDGMENTS

This work was partly supported by a NATO Linkage Grant No. LG 971803. We thank LLB (Laboratoire Léon-Brillouin) for providing the PRISM experimental facility. The support of EU through the Access to Research Infrastructure action of the Improving Human Potential Program is also acknowledged.

APPENDIX

The magnetization, m , within the molecular field approximation is the solution of the equation

$$m - M_s B_f(H, T, \gamma m / M_s) = m - M_s B_f(H/T, m T_c / M_s T) = 0, \quad (\text{A1})$$

where M_s is the saturation magnetization, γ is the molecular field constant

$$\gamma = 3kT_c J(J+1)g\mu_B M_s, \quad (\text{A2})$$

and B_f is the Brillouin function. Equation (A1) for a given external field can be solved numerically to give the magnetization at different temperatures i.e.

$$m(T, T_c) = M_s f(T, T_c), \quad f(T=0, T_c) = 1. \quad (\text{A3})$$

For a molecular field distribution the magnetization will be given as

$$m(T) = \int p(\gamma)m(\gamma,T)d\gamma = \int p(T_c)m(T,T_c)dT_c, \quad (\text{A4})$$

where $p(\gamma)$ is a probability function and the change of variables from γ to T_c has been done by using Eq. (A2). Approximating the probability function with a rectangular one we have

$$\begin{aligned} m(T, T_{c1}, T_{c2}) &= \int_{T_{c1}}^{T_{c2}} m(T, T_c) dT_c = M_s \int_{T_{c1}}^{T_{c2}} f(T, T_c) dT_c \\ &= M_s g(T, T_{c1}, T_{c2}). \end{aligned} \quad (\text{A5})$$

If there are more than one molecular field distribution equation (A5) can be easily generalized and for the case of two distributions ($p_\alpha(\gamma), p_\beta(\gamma)$) can be written as

$$M(T) = M_s^\alpha g(T, T_{c1}^\alpha, T_{c2}^\alpha) + M_s^\beta g(T, T_{c1}^\beta, T_{c2}^\beta). \quad (\text{A6})$$

The normalized to unity magnetization is given as

$$\mu(T) = \mu_s^\alpha g(T, T_{c1}^\alpha, T_{c2}^\alpha) + \mu_s^\beta g(T, T_{c1}^\beta, T_{c2}^\beta), \quad (\text{A7})$$

where

$$\mu_s^\alpha = \frac{M_s^\alpha}{M_s^\alpha + M_s^\beta}. \quad (\text{A8})$$

The scattering length density (SLD), ρ , is defined as

$$\rho = Nb, \quad (\text{A9})$$

where N is the atomic number density and b is the neutron scattering length of an atom (or f for x rays). When an in-

terface AB (B layer is on the top of A) at depth z_0 is sharp the derivative of the SLD at the interface is given by

$$\left. \frac{d\rho}{dz} \right|_{z=z_0} = (\rho_B - \rho_A) \delta(z_0).$$

For a rough interface the derivative of the xy plane average of the SLD may be represented by a Gaussian (Ref. 49), i.e.

$$\frac{d\rho}{dz} = (\rho_B - \rho_A) \frac{1}{\sqrt{2\pi}\sigma_A} \exp\left(-\frac{z-z_0}{2\sigma_A^2}\right),$$

which gives the SLD versus depth profile of the sample

$$\rho(z) = \rho_A + \frac{\rho_B - \rho_A}{2} \left[1 + \operatorname{erf}\left(\frac{z-z_0}{\sqrt{2}\sigma_A}\right) \right], \quad (\text{A10})$$

and σ is the roughness value which is determined by the least squares fitting to the experimental reflectivity data. The extent of the interface between layers B and A is around $2\sigma_A$.

Using the above definition of the roughness the thickness of region α in Fig. 4 is calculated by the equation

$$\mu_s^\alpha = \frac{1}{M_{Gd}} \int_{z_1}^{z_1+D_\alpha} \mu(z) dz, \quad M_{Gd} = \int_{z_1}^{z_1+D_{Gd}} \mu(z) dz, \quad (\text{A11})$$

where $\mu(z)$ is the magnetization profile (Fig. 4), z_1 is the depth at which the Gd layer starts and D_{Gd} is its thickness. μ_s^α is given by the equation (A8) and has the value of 0.38 (see legend of Fig. 5).

*Corresponding author. Email address: bacze@ifpan.edu.pl, Fax: +48 (22) 843-13-31

¹P. Pouloupoulos, A. Scherz, F. Wilhelm, H. Wende, and K. Baberschke, Phys. Status Solidi A **189**, 293 (2002).

²H. Wende, A. Scherz, F. Wilhelm, and K. Baberschke, J. Phys.: Condens. Matter **15**, S547 (2003).

³Li Yi, C. Polaczyk, J. Kapoor, F. Klose, F. Mezei, and D. Riegel, Physica B **234**, 492 (1997).

⁴Y. Li, C. Polaczyk, J. Kapoor, and D. Riegel, J. Magn. Magn. Mater. **165**, 165 (1997).

⁵A. Broddefalk, P. Nordblad, P. Blomquist, P. Isberg, R. Wäppling, O. Le Bacq, and O. Eriksson, J. Magn. Magn. Mater. **241**, 260 (2002).

⁶B. Kalska, P. Blomquist, L. Häggström, and R. Wäppling, Europhys. Lett. **53**, 395 (2001).

⁷V. L. Aksnov, Yu. V. Nikitenko, V. V. Proglyado, M. A. Andreeva, B. Kalska, L. Häggström, and R. Wäppling, J. Magn. Magn. Mater. **258**, 332 (2003).

⁸B. A. Hamad and J. M. Khalifeh, Surf. Sci. **481**, 33 (2001).

⁹A. Scherz, H. Wende, K. Baberschke, J. Minar, D. Benea, and H. Ebert, Phys. Rev. B **66**, 184401 (2002).

¹⁰A. Scherz, H. Wende, P. Pouloupoulos, J. Lindner, K. Baberschke, F. Wilhelm, N. B. Brookes, P. Blomquist, and R. Wäppling Phys. Rev. B **64**, 180407(R) (2001).

¹¹P. Nordblad, A. Broddefalk, R. Mathieu, P. Blomqvist, O. Eriksson, and R. Wäppling, Physica B **327**, 344 (2003).

son, and R. Wäppling, Physica B **327**, 344 (2003).

¹²O. Eriksson, L. Bergqvist, E. Holmström, A. Bergman, O. Le Bacq, S. Frota-Pessoa, B. Hjörvarsson, and L. Nordström, J. Phys.: Condens. Matter **15**, S599 (2003).

¹³M. Farle, A. N. Anisimov, K. Baberschke, J. Langer, and H. Maletta, Europhys. Lett. **49**, 658 (2000).

¹⁴O. Le Bacq, B. Johansson, and O. Eriksson, J. Magn. Magn. Mater. **226**, 1724 (2001).

¹⁵J. Izquierdo, A. Vega, O. Elmouhssine, H. Dreyse, and C. Demangeat, Phys. Rev. B **59**, 14510 (1999).

¹⁶R. Coehoorn, J. Magn. Magn. Mater. **151**, 341 (1995).

¹⁷M. A. Tomaz, W. J. Antel Jr., W. L. O'Brien, and G. R. Harp, J. Magn. Magn. Mater. **9**, L179 (1997).

¹⁸M. M. Schwickert, R. Coehoorn, M. A. Tomaz, E. Mayo, D. Lederman, W. L. O'Brien, Tao Lin, and G. R. Harp, Phys. Rev. B **57**, 13681 (1998).

¹⁹A. Scherz, P. Pouloupoulos, H. Wende, G. Ceballos, K. Baberschke, and F. Wilhelm, J. Appl. Phys. **91**, 8760 (2002).

²⁰A. Scherz, P. Pouloupoulos, R. Nunthel, J. Lindner, H. Wende, F. Wilhelm, and K. Baberschke, Phys. Rev. B **68**, 140401(R) (2003).

²¹R. E. Camley and R. L. Stamps, J. Phys.: Condens. Matter **5**, 3727 (1993).

²²D. Weller, S. F. Alvarado, W. Gudat, K. Schroder, and M. Campagna, Phys. Rev. Lett. **54**, 1555 (1985).

- ²³J. Colino, J. P. Andres, J. M. Riveiro, J. L. Martinez, C. Prieto, and J. L. Sacedón, *Phys. Rev. B* **60**, 6678 (1999).
- ²⁴D. Haskel, G. Srajer, J. C. Lang, J. Pollmann, C. S. Nelson, J. S. Jiang, and S. D. Bader, *Phys. Rev. Lett.* **87**, 207201 (2001).
- ²⁵D. Haskel, G. Srajer, Y. Choi, D. R. Lee, J. C. Lang, J. Meersschaut, J. S. Jiang, and S. D. Bader, *Phys. Rev. B* **67**, 180406(R) (2003).
- ²⁶J. P. Andres, L. Chico, J. Colino, and J. M. Riveiro, *Phys. Rev. B* **66**, 094424 (2002).
- ²⁷E. Meltchakov, H.-Ch. Mertins, M. Scheer, S. Di Fonzo, W. Jark, and F. Schäfers, *J. Magn. Magn. Mater.* **240**, 550 (2002).
- ²⁸A. Pogorily, E. Shypil, and C. Alexander, *J. Magn. Magn. Mater.* (unpublished).
- ²⁹C. F. Majkrzak, J. W. Cable, J. Kwo, M. Hong, D. B. McWhan, Y. Yafet, J. V. Waszczak, and C. Vettier, *Phys. Rev. Lett.* **56**, 2700 (1986).
- ³⁰<http://www-llb.cea.fr/prism/programs/simulreflec/simulreflec.html>, version 1.9.
- ³¹P. Pankowski, L. T. Baczewski, T. Story, A. Wawro, K. Mergia, and S. Messoloras, *Phys. Status Solidi C* **1**, 405 (2004).
- ³²J. Grobner, D. Kevorkov, and R. Schmid-Fetzer, *Zashch. Met.* **92**, 22 (2001).
- ³³P. Pankowski, S. Pizzini, J. B. Pelka, A. Wawro, and L. T. Baczewski, *J. Alloys Compd.* **362**, 56 (2004).
- ³⁴M. Eizenberg, R. D. Thompson, and K. N. Tu, *J. Appl. Phys.* **53**(10), 6891 (1982).
- ³⁵R. Thomson, M. Eizenberg, and K. N. Tu, *J. Appl. Phys.* **52**(11), 6763 (1981).
- ³⁶V. O. Vaskovskiy, A. V. Svalov, A. V. Gorbunov, N. Schegoleva, and S. M. Zadvorkin, *Physica B* **315**, 143 (2002).
- ³⁷V. L. Moruzzi, P. M. Marcus, and P. C. Pattnaik, *Phys. Rev. B* **37**, 8003 (1988).
- ³⁸G. Bihlmayer, T. Asada, and S. Blugel, *Phys. Rev. B* **62**, R11937 (2000).
- ³⁹V. L. Moruzzi and P. M. Marcus, *Phys. Rev. B* **42**, 8361 (1990).
- ⁴⁰S. Bouarab, H. Nait-Laziz, C. Demangeat, A. Mokrani, and H. Dreyse, *Phys. Rev. B* **46**, 889 (1992).
- ⁴¹A. C. Jenkins and W. M. Temmerman, *J. Magn. Magn. Mater.* **198**, 584 (1999).
- ⁴²Y. Huttel, G. van der Laan, T. K. Johal, N. D. Telling, and P. Bencok, *Phys. Rev. B* **68**, 174405 (2003).
- ⁴³N. Jiko, K. Mibu, and L. T. Baczewski, *IEEE Trans. Magn.* **41**(10), 3352 (2005).
- ⁴⁴B. N. Harmon and A. J. Freeman, *Phys. Rev. B* **10**, 1979 (1974).
- ⁴⁵O. S. Anilturk and A. R. Koymen, *Phys. Rev. B* **68**, 024430 (2003).
- ⁴⁶F. Huang, G. J. Mankey, M. T. Kief, and R. F. Willis, *J. Appl. Phys.* **73**, 6760 (1993); J. S. Jiang, D. Davidovic, Daniel H. Reich, and C. L. Chien, *Phys. Rev. Lett.* **59**, 2596 (1987).
- ⁴⁷R. Zhang and R. F. Willis, *Phys. Rev. Lett.* **86**, 2665 (2001).
- ⁴⁸M. Taborelli, R. Allenspach, G. Boffa, and M. Landolt, *Phys. Rev. Lett.* **56**, 2869 (1986).
- ⁴⁹Xiao-Lin Zhou and Sow-Hsin Chen, *Phys. Rep.* **223**, (1995).